ISSN 1674-1056
http://cpb.iphy.ac.cn
http://iopscience.iop.org/cpb
中国物理 B
Chinese Physics
中国物理 Chinese Physics B

Temporal pulsed x-ray response of CdZnTe:In detector

Rong-Rong Guo(郭榕榕), Ya-Dong Xu(徐亚东), Gang-Qiang Zha(查钢强), Tao Wang(王涛), Wan-Qi Jie(介万奇)

Citation: Chin. Phys. B . 2018, 27(12): 127202. **doi:** 10.1088/1674-1056/27/12/127202
Journal homepage: http://cpb.iphy.ac.cn; http://iopscience.iop.org/cpb

What follows is a list of articles you may be interested in

---

win boundary dominated electric field distribution in CdZnTe detectors

Jiangpeng Dong(董江鹏), Wanqi Jie(介万奇), Jingyi Yu(余竞一), Rongrong Guo(郭榕榕), Christian Teichert, Kevin-P Gradwohl, Bin-Bin Zhang(张滨滨), Xiangxiang Luo(罗翔祥), Shouzhi Xi(席守智), Yadong Xu(徐亚东)

Chin. Phys. B . 2018, 27(11): 117202. **doi:** 10.1088/1674-1056/27/11/117202

Modeling capacitance–voltage characteristic of TiW/p-InP Schottky barrier diode

Yi-Dong Wang(王一栋), Jun Chen(陈俊)

Chin. Phys. B . 2018, 27(9): 097203. **doi:** 10.1088/1674-1056/27/9/097203

Room-temperature large photoinduced magnetoresistance in semi-insulating gallium arsenide-based device

Xiong He(何雄), Zhi-Gang Sun(孙志刚)

Chin. Phys. B . 2018, 27(6): 067204. **doi:** 10.1088/1674-1056/27/6/067204

First-principles hybrid functional study of the electronic structure and charge carrier mobility in perovskite $CH_3NH_3SnI_3$

Li-Juan Wu(伍丽娟), Yu-Qing Zhao(赵宇清), Chang-Wen Chen(陈畅文), Ling-Zhi Wang(王琳芝), Biao Liu(刘标), Meng-Qiu Cai(蔡孟秋)

Chin. Phys. B . 2016, 25(10): 107202. **doi:** 10.1088/1674-1056/25/10/107202

Effect of de-trapping on carrier transport process in semi-insulating CdZnTe

Guo Rong-Rong, Jie Wan-Qi, Zha Gang-Qiang, Xu Ya-Dong, Feng Tao, Wang Tao, Du Zhuo-Tong

Chin. Phys. B . 2015, 24(6): 067203. **doi:** 10.1088/1674-1056/24/6/067203

Temporal pulsed x-ray response of CdZnTe: In detector*

Rong-Rong Guo(郭榕榕)[1,2], Ya-Dong Xu(徐亚东)[2,†], Gang-Qiang Zha(查钢强)[2], Tao Wang(王涛)[2], and Wan-Qi Jie(介万奇)[2]

[1] School of Optoelectronic and Communication Engineering, Xiamen University of Technology, Xiamen 361024, China
[2] State Key Laboratory of Solidification Processing, Northwestern Polytechnical University (NWPU), Xi'an 710072, China

(Received 17 August 2018; revised manuscript received 26 September 2018; published online 10 November 2018)

The temporal response of cadmium-zinc-telluride (CZT) crystals is evaluated at room temperature by using an ultrafast-pulsed x-ray source. The dynamics of carrier relaxation in a CZT single crystal is modeled at a microscopic level based on a multi-trapping effect. The effects of the irradiation flux and bias voltage on the amplitude and full width at half maximum (FWHM) of the transient currents are investigated. It is demonstrated that the temporal response process is affected by defect level occupation fraction. A fast photon current can be achieved under intense pulsed x-ray irradiation to be up to 2.78×10^9 photons $\mathrm{mm}^{-2}\cdot\mathrm{s}^{-1}$. Meanwhile, it is found that high bias voltage could enhance carrier detrapping by suppressing the capture of structure defects and thus improve the temporal response of CZT detectors.

Keywords: CdZnTe, ultrafast-pulsed x-rays, transient current, charge carrier

PACS: 72.80.Ey, 73.50.Gr, 73.61.Ga, 72.20.Jv **DOI:** 10.1088/1674-1056/27/12/127202

1. Introduction

In order to improve the early stage detection and diagnosis of diseased tissue, such as tumors or breast cancer, high-quality gamma and x-ray detectors are required in medical diagnostics and therapy equipment. For these applications, the typical x-ray flux could reach values as high as 200 MHz/mm^2–2000 MHz/mm^2. It is therefore a great challenge to operate the detectors in pulse mode. So far, scintillation detectors coupled with photo-detectors have been mostly employed in timing measurements, such as in nuclear physics experiment diagnosis and in positron emission tomography (PET) imaging.[1] Unfortunately, the energy and spatial resolution of scintillators are usually limited, especially in the case where the scintillator size needs to be reduced.[2] To overcome this shortcoming, CdZnTe (CZT) detectors with higher stopping power, compact size and better spatial resolution are becoming attractive for various hard x-ray and soft γ-ray imaging applications.[3–5] However, the development of CZT detectors for medical imaging system is challenged by a number of factors, particularly the inherent defects within bulk crystals. Trapping, detrapping and recombination through those defects can significantly deteriorate the detector performance under the high flux pulse model, thus inducing afterglow, ghosting and polarization effects.

Thus, an in-depth understanding of the temporal response mechanism of CZT detectors is required in order to record x-ray or γ-ray emission accurately. There have been a few studies of exploring the temporal response of CZT detectors. For instance, ^{241}Am α–γ coincidence[6] and high energy pulsed x-ray photons[7] have been utilized to investigate the temporal properties of CZT detectors. These measurements suggested that CZT has a time resolution on the order of a few nanoseconds and can be improved by using digital signal processing.[8,9] Du *et al.*[10] have suggested that the temporal response of CZT may be unstable under intense irradiation. Bale *et al.*[11] reported the lateral polarization effect generated in CZT detectors, which were fabricated from crystals with low hole transport properties, due to the hole trapping when exposed to the continuous high-flux x-rays.

In contrast to most of the existing literature, the present work focuses on the corresponding properties of CZT under ultrafast pulsed x-rays with high intensity. Specifically, the carrier recombination, trapping and detrapping processes through defect levels in the carrier transport process are discussed to explain the temporal relaxation process. Based on that, a mechanism of polarization under high x-ray flux and the effect of bias voltage on temporal response are proposed, to provide a guide for optimizing CZT material and detector design.

2. Experiment

High-resistivity indium-doped $Cd_{0.9}Zn_{0.1}Te$ crystals grown by the modified vertical Bridgman method under the Terich condition[12] have been used in this study. The samples were cut from the as-grown ingots with dimensions of 10 mm×10 mm×1 mm and fabricated into planar structures

*Project supported by the National Natural Science Foundation of China (Grant Nos. 51702271 and U1631116), the Young and Middle-aged Teachers Education and Scientific Research Foundation of Fujian Province, China (Grant No. JAT170407), the High Level Talent Project of Xiamen University of Technology, China (Grant No.YKJ16016R), and the Fund of the State Key Laboratory of Solidification Processing in NWPU, China (Grant No. SKLSP201741).

†Corresponding author. E-mail: xyd220@nwpu.edu.cn

© 2018 Chinese Physical Society and IOP Publishing Ltd

with Au contacts. The typical leakage current for the devices was 2 nA–8 nA at an electric field strength of 1000 V/cm. The electron mobility lifetime product was determined to be 1.9×10^{-3} cm^2·V^{-1} by ^{241}Am coincident 5.48-MeV alpha particle response measurement.

For temporal pulsed x-ray response measurement, the CZT detector was biased by using a commercial DC power supply (Keithley 248). The induced current signal from the detector was recorded directly by a digital oscilloscope (Tektronix TDS 4104, 1 GHz, 5 GS/s) connected through a 50-Ω load resistor. The schematic diagram of the setup used for the temporal response measurements are shown in Ref. [13] . Ultrafast x-rays were produced from a sub-nanosecond repetition rate pulsed hard x-ray generator with a changeable tube voltage from 200 kV to 350 kV. The repetition frequencies of 1, 2, 10 or 100 Hz could be achieved. A tunable duration of $\sim$ 200 picoseconds was obtained by using a peaking–chopping switch. A special attenuation film was positioned at the emission port to partially absorb the high energy x-rays. The majority of the emission photons had energies in a range of 40 keV–70 keV,[13] which results in the variation of the depth of interaction (DOI) in CZT detector. The incident x-ray flux of each pulse is approximately 10^9 photons mm^{-2} at a distance of 1 meter from the emission port, which is proportional to $1/r^2$, where r is the distance from the beam port. All measurements were conducted at room temperature.

3. Results and discussion

3.1. Fundamental principle of pulsed x-rays measurements

Since the mean penetration depth of the x-rays in CZT ranges from 90 μm to 400 μm, the majority of the photons will be absorbed by the 1-mm-thick CZT samples. Plenty of electron–hole (eh) pairs are generated in the bulk CZT crystal by photoelectric effect. Under the influence of the electric field, the electrons and holes will be separated from each other and drift toward anode and cathode, respectively, which forms the current measured in the external circuit. Figure 1(a) shows a typical photo-response transient current waveform of CZT, which is produced on the cathode side under a bias of 300 V. A sharp rise to a maximum value at the beginning of the exposure is observed. The rise time (τ_r) is calculated to be about 2.2 ns, which depends on the implosion time of x-ray and the intrinsic response time of the detector. The tunable duration of x-ray is $\sim$ 200 ps, which is much shorter than that of CZT detector. Thus, the rise time of the response transient waveform can be considered as to be an manifestation of the time-response properties of the CZT detector.

After reaching maximum amplitude, the current waveform starts to decrease exponentially back to the baseline. Figure 1(b) schematically shows the formation of the pulsed x-ray-induced transient waveform. Since the pulsed x-rays are non-monochromic, the depths of interaction in CZT crystal are random and uncertain. Thus, the transient current waveforms become dispersive and no transit time is discernable.

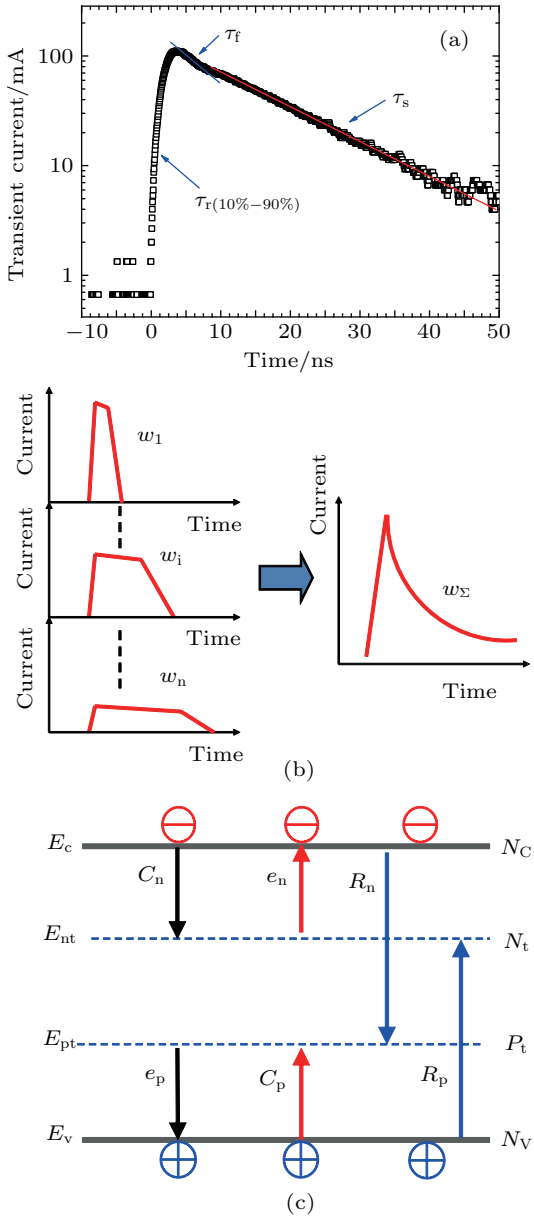


Fig. 1. (color online) (a) Typical transient current waveform for CZT under bias voltage of 300 V, (b) schematic illustration of the formation of pulsed x-rays induced transient current waveform, and (c) major process of carrier restored by trapping $C_{n(p)}$, detrapping $e_{n(p)}$, and recombination $R_{n(p)}$.

The transient current relaxation process is associated with the carrier drift, trapping and recombination, which consists of a fast (τ_f) component and a slow (τ_s) component, as shown in Fig. 1(a). It is well documented that defect levels are inevitable, which can significantly change the transient current waveform by trapping and recombination effects.[14] The multiple-trapping process[15] describes this dynamic of carriers restoring to equilibrium, as illustrated in Fig. 1(c). For simplicity, only two trap levels, denoted as E_{nt} and E_{pt}, are considered for electrons and holes, respectively. In the CZT

crystal grown under the Terich condition, the deep-level defect Te_{Cd} with the second ionization energy of ~ 0.59 eV and V_{Cd} with the second ionization energy of ~ 0.43 eV have been well known as the electron and hole trap centers,[14] respectively, which may dominate this relaxation process. Without considering the diffusion effect, the basic one-dimensional transportation equations for the free electron density $n(x,t)$ and trapped charge density $n_t(x,t)$ in CZT crystal are as follows:

$$\frac{\partial n}{\partial t} = -\mu_n E \frac{\partial n}{\partial x} - R_n n - C_n n + e_n n_t, \quad (1)$$

$$\frac{\partial n_t}{\partial t} = C_n n - e_n n_t - R_p p, \quad (2)$$

where x is the distance from one electrode, E is the electric field which can be determined by the Poisson equation and n_t is the density of electrons that are trapped in the defect levels. The electron (hole) recombination rate $R_{n(p)}$, the electron capture rate C_n and the electron emission rate e_n are given by,[16,17]

$$R_n = p_t \sigma_{nr} v_{th}, \quad (3)$$

$$R_p = n_t \sigma_{pr} v_{th}, \quad (4)$$

$$C_n = (N_t - n_t)\sigma_{nt} v_{th}, \quad (5)$$

$$e_n = N_c \sigma_{nt} v_{th} \exp(-(E_c - E_{nt})/kT), \quad (6)$$

where $\sigma_{n(p)r}$ is the electron (hole) recombination cross section, σ_{nt} is the electron capture cross section, N_t is the total density of electron trap levels and v_{th} is the thermal velocity of carriers.

These equations predict that the net rate of carrier is a function of defect-level occupation fraction. After the x-ray is terminated, all the trapping centers are filled and the net flows of carrier at defect levels are nearly zero. The electrons in the conduction band will recombine rapidly at a high density of excess carriers, which plays an important role in the fast component of the photo-response waveforms. As the excess carriers in conduction band decay sufficiently, the trapped carriers will be thermally reemitted back into conduction band simultaneously, which dominates the slow component of the photo-response waveforms.[14] By the subsectional fitting of the transient current with single exponential, the fast decay time τ_f and the slow decay time τ_s are calculated to be 9.17 ns and 14.01 ns, respectively.

3.2. Effect of irradiation flux

To determine the effect of the irradiation flux on the temporal response performance, the transient current waveform of CZT is obtained as a function of the distance from the x-ray source (r) at an identical bias of 150 V, as seen in Fig. 2(a). The full width at half maximum (FWHM) of the transient waveform is introduced to evaluate the effective transit time in relaxation process under the uniform pulsed x-ray injection condition.[18] The amplitude and FWHM of the photo-response current waveform are measured and plotted versus x-ray flux, as shown in Figs. 2(b) and 2(c), respectively. A growing x-ray flux will result in the increase of the number of eh pairs and consequently the amplitude of transient current, which accords well with the experimental data. The photo-response current amplitude increases linearly under low x-ray flux. It demonstrates that the electrical filed is nearly uniform within the CZT detector under lower x-ray flux. The effective electron velocity υ_{eff} can be determined by $\upsilon_{eff} = \mu_e U/L$, where U is the bias voltage and L is the detector thickness. However, with the flux increasing beyond 2.78×10^9 photons mm^{-2}, it becomes sublinear. The polarization will occur with the increase of the carrier trapping under higher x-ray flux. The effective electron velocity υ_{eff} can be evaluated from

$$\upsilon_{eff} = \frac{\mu_e U}{L}\left(\frac{\tau_e}{\tau_e + \tau_D}\right),$$

where τ_e and τ_D are the electron trapping time and detrapping time, respectively.[11] In this case, the carrier trapping effect significantly reduces the effective electron velocity. The additional space charge originating from trapped photo-carriers is accumulated at deep levels. Once the space charge exceeds the critical value, the net effective field across the device is significantly reduced, leading ultimately to the electric field to collapse in the detector.[19,20] Eventually, a dead layer will form inside the detector, thus significantly reducing the charge collection efficiency.

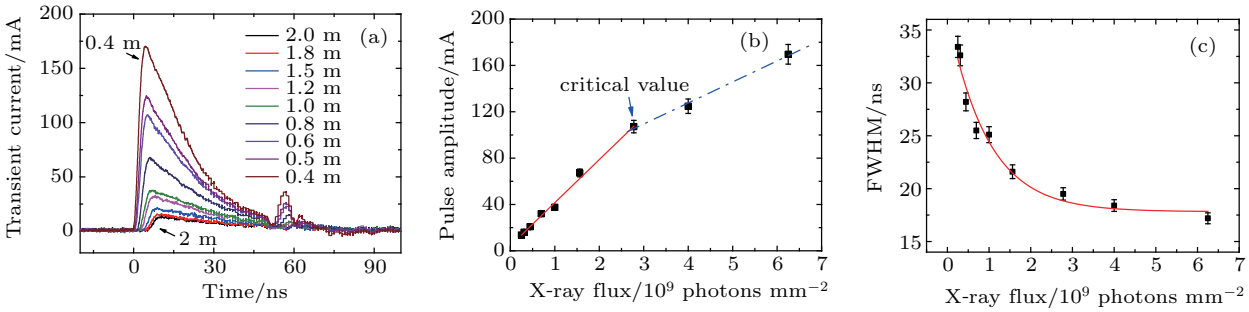


Fig. 2. (color online) (a) Temporal response waveforms as a function of distance r at an identical bias of 150 V, (b) signal amplitude versus x-ray flux, (c) plot of FWHM of signals versus x-ray flux, with solid squares representing experimental data and red solid lines referring to linear and exponential fitting, respectively.

The FWHM of the current waveform decreases with x-ray flux increasing, as seen in Fig. 2(c). It suggests that the concentration of excess carriers influences the FWHM by the fluctuation of defect occupation fraction. The excess carriers are more likely to recombine with each other rapidly when the excess carrier concentration is high enough to fill all the trap centers. Thus, the FWHM is smaller under higher x-ray flux. However, the FWHM of the transient current waveform will be broadened by the carrier detrapping effect, since carrier concentration in conduction band is deficient under the low flux irradiation.

3.3. Bias voltage-dependent measurements

The polarization effect is strongly affected by x-ray flux, temperature and bias voltage. Based on the above results, the CZT detector is located at a distance of 1 m from the x-ray beam port to avoid the space charge accumulation effect. The effect of bias voltage on temporal x-ray response is studied. Generally, the variation in the x-ray flux can be neglected at a fixed distance. Thus, the number of eh pairs generated by photoelectric effect is constant. Figure 3(a) shows the typical bias dependence of photo-response current waveform. The good linearity is shown between the transient current amplitude and bias voltage, which confirms that no obvious space charge accumulation effect is present as seen in Fig. 3(b).

The fall time of the transient waveform signal decreases with the bias voltage increasing. Figure 3(c) shows the FWHM of the transient current waveform as a function of bias voltage. A fitting to the experimental data shows that the FWHM is inversely proportional to the bias voltage. Significant carriers trapping in CZT crystal at lower bias voltage will result in a reduction in the transient current intensity and prolong the transit time. Thus, the FWHM is broadened at a lower bias voltage. However, with the increase of the bias voltage, the slow decay time (τ_s) decreases from 40 ns to 11.62 ns. As mentioned above, the slow component of transient current is dominant by carrier detrapping effect. It indicates that the bias voltage enhances the carrier emission from trap center, and thus reduces the τ_s. This phenomenon has been well described by the Poole–Frenkel effect.[21]

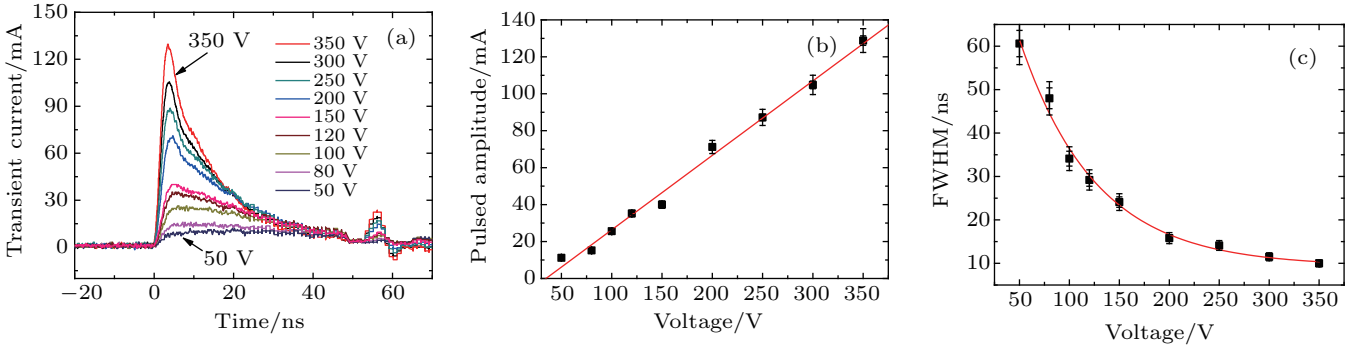


Fig. 3. (color online) (a) Temporal response waveforms as a function of bias voltage under similar irradiation flux ($r = 1$ m), (b) bias dependence of signals amplitude, (c) FWHM of the signals versus bias voltages, with solid squares representing experimental data and red solid lines denoting linear and exponential fit, respectively.

On the other hand, the charge transport behaviors are also significantly influenced by structural defects such as Te inclusions.[22] The charge cloud spreads when it drifts towards the electrode, with its radius $r(t)$ being as a function of detector bias as follows:[23]

$$r(t) = 1.15\sqrt{\frac{2k_{\mathrm{B}}Td(t)D}{qV}}, \tag{7}$$

where $d(t)$ is the drift distance of the charge cloud, k_{B} is Boltzmann's constant, D is the detector width, T is the temperature, q is the charge of the carriers and V is the detector bias. An increase in the bias voltage will cause an associated decrease in the charge cloud radius r. This means that the carriers are less likely to become trapped or scattered, leading the "charge carrier cloud" transit time to decrease. In turn, the decrease of FWHM of the transient current waveform is observed to be a function of applied bias.

4. Conclusions

The temporal pulsed x-ray response of CZT crystal is evaluated at room temperature. The rise time of transient current is found to be 2 ns, indicating the excellent time resolution of the CZT detector. The relaxation process of transient current is modeled at a microscopic level and described by the multi-trapping effect. It is proposed that the fast decay part is dominated by a recombination process while the slow decay part is controlled by a carrier detrapping effect. The results of flux-dependent transient current measurement further confirm that the FWHM of transient current is affected by the defect occupation fraction.

The relatively low sensitivity to pulsed x-ray can be explained in terms of a dead layer induced by a space charge accumulation effect, which significantly collapses the electric field. The critical value of polarization is $\sim 2.78 \times 10^9$ photons $\mathrm{mm}^{-2}\cdot\mathrm{s}^{-1}$ in CZT crystal. To further improve the temporal response of CZT detectors, high bias voltage is used

to enhance carrier detrapping and alleviate the capturing from structural defects.

Acknowledgment

The authors would like to thank the team at the Sub-nanosecond Reprate Pulse Hard x-ray Generator Radiation Facility of NINT for providing beam time. The authors would like to give special thanks to Drs. Xiaochuan Zhao and Chunlei Su from the Institute of Nuclear Physics and Chemistry, China Academy of Engineering Physics, for the fruitful discussion on pulse hard x-ray measurements.

References

[1] Tai Y C, Ruangma A, Rowl, D, Siegel S, Newport D F, Chow P L and Laforest R 2005 *J. Nucl. Med.* **46** 455
[2] Van Loef E V D, Dorenbos P, Van Eijk C W E, Krämer K and Güdel H U 2001 *Appl. Phys. Lett.* **79** 1573
[3] Schlesinger T E, Toney J E, Yoon H, Lee E Y, Brunett B A, Franks L and James R B 2001 *Mater. Sci. Eng. R Rep.* **32** 103
[4] Herzog B A, Buechel R R, Katz R, Brueckner M, Husmann L, Burger I A, Pazhenkottil A P, Valenta I, Gaemperli O, Treyer V and Kaufmann P A 2010 *J. Nucl. Med.* **51** 46
[5] Hong J, Allen B, Grindlay J, Barthelemy S, Baker R, Garson A, Krawczynski H, Apple J, Clevel and W H 2011 *Nucl. Instrum. Methods Phys. Res. Sect. A* **654** 361
[6] Okada Y, Takahashi T, Sato G, Watanabe S, Nakazawa K and Mori K 2002 *IEEE Trans. Nucl. Sci.* **49** 1986
[7] Glasser F, Gerbe V, OuvrierBuffet P, Accensi M, Girard J L, Renaud M and GerstenMayer J L 2001 *Nucl. Instrum. Methods Phys. Res. Sect. A* **458** 544
[8] Nakhostin M, Ishii K, Kikuchi Y, Matsuyama S, Yamazaki H and Torshabi A E 2009 *Nucl. Instrum. Methods Phys. Res. Sect. A* **606** 681
[9] Nakhostin M, Walker P M and Sellin P J 2010 *Nucl. Instrum. Methods Phys. Res. Sect. A* **621** 506
[10] LeBlanc J, Possin G E, Yanoff B D and Bogdanovich S 2003 *IEEE Trans. Nucl. Sci.* **50** 1031
[11] Bale D S, Soldner S A and Szeles C 2008 *Appl. Phys. Lett.* **92** 82101
[12] Xu Y, Jie W, Sellin P J, Wang T, Fu L, Zha G and Veeramani P 2009 *IEEE Trans. Nucl. Sci.* **56** 2808
[13] Zhao X C, Ouyang X P, Xu Y D, Han H T, Zhang Z C, Wang T, Zha G Q and Ouyang X 2012 *AIP Adv.* **2** 12162
[14] Guo R, Jie W, Wang N, Zha G, Xu Y, Wang T and Fu X 2015 *J. Appl. Phys.* **117** 94502-1
[15] Tiedje T 1984 *Semiconductors and Semimetals*, Vol. 21 (Academic Press) pp. 207–238
[16] Shockley W and Read W T 1952 *Phys. Rev.* **87** 835
[17] Elhadidy H, Franc J, Moravec P, Höschl P and Fiederle M 2007 *Semicond. Sci. Technol.* **22** 537
[18] Zhou J and Shimizu T 1993 *Solid State Commun.* **88** 173
[19] Belas E, Hoschl P, Moravec P, Praus P, Franc J, Grill R and Kuba J 2011 *Nucl. Instrum. Methods Phys. Res. A* **633** 100
[20] Siffert P, Berger J, Scharager C, Cornet A, Stuck R, Nucleaires C D R, Serreze H B, Wald F V, Tyco M and Energy S 1976 *IEEE Trans. Nucl. Sci.* **NS-23** 159
[21] Ottaviani G, Canali C, Jacoboni C, Quaranta A A and Zanio K 1973 *J. Appl. Phys.* **44** 360
[22] Carini G A, Bolotnikov A E, Camarda G S, Wright G W, James R B and Li L 2006 *Appl. Phys. Lett.* **88** 143515
[23] Iniewski K, Chen H, Bindley G, Kuvvetli I and Jorgensen C B 2007 *IEEE Nucl. Sci. Symp. Conf. Rec.* 4608